

Magnetars: Time Evolution, Superfluid Properties, and Mechanism of Magnetic Field Decay

P. Arras¹, A. Cumming², C. Thompson³

ABSTRACT

We calculate the coupled thermal evolution and magnetic field decay in relativistic model neutron stars threaded by superstrong magnetic fields ($B > 10^{15}$ G). Our main goal is to evaluate how such “magnetars” evolve with time and how field decay modifies the transitions to core superfluidity and cooling dominated by surface X-ray emission. Observations of a thermal X-ray spectral component and fast timing noise place strong constraints on the presence of a superfluid core. We find that the transition to core superfluidity can be significantly delayed by field decay in the age range $\sim 10^3 - 10^5$ yrs. The mechanism of Hall drift is related to the stability of the core magnetic field, and to currents flowing outward through the crust. The heating effect is enhanced if it is continuous rather than spasmodic. Condensation of a heavy element layer at the surface is shown to cause only modest changes in the outward conduction of heat.

Subject headings: magnetic fields: stars – neutron stars: general

1. Introduction

Observations of the Soft Gamma Repeaters and Anomalous X-ray Pulsars have revealed a rich phenomenology of transient X-ray emission and torque variability. Some members of the first group occasionally emit enormously bright X-ray flares (Hurley 2000), which are followed by transient periods of decaying X-ray flux. The unified nature of the SGRs and AXPs is indicated by the detection of ~ 0.1 s hard-spectrum X-ray bursts from two AXPs (Gavriil et al. 2002; Kaspi et al. 2003). This variable X-ray emission is now generally

¹Kavli Institute for Theoretical Physics, University of California, Santa Barbara, CA

²Department of Astronomy and Astrophysics, University of California, Santa Cruz, CA

³Canadian Institute for Theoretical Astrophysics, 60 St. George St., Toronto, ON M5S 3H8

believed to be powered by the decay of an ultrastrong magnetic field (Thompson & Duncan 1996; Colpi, Geppert & Page 2000).

Two sub-classes of these objects have emerged recently: those which maintain a fairly steady X-ray luminosity over two decades or longer; and a less conspicuous group (not necessarily smaller in total numbers) in which one sees transitions to and from very low levels of persistent X-ray emission over a period of months to years (Torii et al. 1998; Kouveliotou et al. 2003; Ibrahim et al. 2003). Objects in the second group are weak burst sources or have not been observed to burst at all.

Some SGRs and AXPs also show strong timing irregularities, which broadly can be divided into i) adiabatic variations in torque over a period of months to years (Kaspi et al. 2001; Woods et al. 2002) and ii) a broad spectrum of timing noise starting from periods as short as $\sim 10^4$ s and upward. Our goal here is to isolate the most important mechanisms by which an ultrastrong magnetic field will contribute to the persistent X-ray emission of these objects (on timescales of years or longer); and also to make deductions about the composition of the star from the appearance of strong timing noise in active burst sources.

2. Basic Modes of Magnetic Field Decay

A decaying magnetic field in a neutron star evolves through a series of equilibrium states, punctuated by the release of elastic stresses in its crust and the excitation of hydrodynamic motions in its liquid core. The crust is too weak to sustain all but modest departures from magnetostatic equilibrium, if $B > 10^{15}$ G. In the case of a purely fluid star that is stabilized against convection in the radial direction, it is generally believed that the equilibrium states of the magnetic field must carry some net helicity, e.g., that the field has both toroidal and poloidal components. Purely poloidal (Flowers and Ruderman 1975) and purely toroidal (Tayler 1973) fields are unstable.

The magnetic field evolves according to the equation

$$\frac{\partial \mathbf{B}}{\partial t} = \nabla \times [(\mathbf{v} + \mathbf{v}_{\text{amb}} + \mathbf{v}_{\text{Hall}}) \times \mathbf{B}] + \frac{\partial \mathbf{B}}{\partial t} \Big|_{\text{fracture}} \quad (1)$$

Here \mathbf{v}_{amb} is the speed with which the magnetic field is advected by the diffusing charged component (electrons/protons) of the neutron star core; $\mathbf{v}_{\text{Hall}} = -\mathbf{J}/en_e$; and \mathbf{v} is the hydrodynamic response of the core to the combined effect of these transport processes. The rigid crust is also subject to sporadic yields and fractures which cause changes in \mathbf{B} (both in crust and core) on short timescales. The star is spherical in a first approximation, and the compositional stratification enforces $v_r = O(\varepsilon_B) \simeq 0$ and $\nabla \cdot \mathbf{v} = O(\varepsilon_B) \simeq 0$ (Reisenegger &

Goldreich 1992). Here $\varepsilon_B = B^2/8\pi P_e$ and P_e is the electron pressure.

The diffusion of charged particles in a normal, degenerate n - p - e plasma is limited by proton-neutron drag at high temperatures (Haensel et al. 1990; Goldreich & Reisenegger 1992, hereafter GR); and at $T < 5 \times 10^8$ K by the rate of relaxation of chemical potential gradients (GR; Pethick 1992). We note here that the n - p collision rate is also reduced dramatically after the transition to proton superconductivity (due to the lower density of quasiparticle excitations near the proton fermi surface). This probably happens early on compared with the $\sim 10^4$ yr lifetime of SGR/AXP activity (e.g. Yakovlev et al. 2001). To calculate the continuing ambipolar diffusion of a magnetic field in a superconducting core, we therefore include only the limiting effects of chemical potential gradients. In this case, the timescale is $t_{\text{amb}}(B, T) \simeq 8\pi n_e^2 (k_B T)^2 / \dot{U}_{\text{Urca}}(\rho, T) B^2$ when the chemical potential imbalance $\Delta\mu \sim B^2/8\pi n_e$ induced by the $\mathbf{J} \times \mathbf{B}/c$ force is much less than $k_B T$. Here \dot{U}_{Urca} is the rate at which beta transformations between neutrons and protons release energy to neutrinos. This rate is strongly modified by Cooper pairing of protons and neutrons, and we include the resulting corrections as tabulated in Yakovlev et al. (2001). For mean fields stronger than several $\times 10^{14}$ G, the magnetic sheaths of the superconducting fluxoids are packed together. Any collective motion of the fluxoids with respect to the protons is strongly inhibited, and we can treat the field as being continuous. In a normal n - p - e core, the heating induced by the decay of the field leads to a direction relation $k_B T \sim \Delta\mu \propto B^2$ between T and B . Given the strong T -dependence of the URCA rates, this causes a strong feedback $t_{\text{amb}} \propto B^{-14}$ on the drift rate above a critical flux density of $\sim 3 \times 10^{15}$ G (Thompson & Duncan 1996).

If the interior magnetic field of a neutron star is helical, then the current density \mathbf{J} and \mathbf{B} both have poloidal components. In a magnetar, closure of this poloidal current inside the star generates a $\mathbf{J} \times \mathbf{B}/c$ force which is strong enough to fracture the crust, thereby twisting up the external magnetic field (Thompson, Lyutikov, & Kulkarni 2002). This mechanism is driven by Hall effect in the crust, through the gradient in electron density with height z . The Hall term in eq. (1) yields $t_{\text{Hall}}^{-1} \equiv B_\phi^{-1} (\partial B_\phi / \partial t) = J_z (\partial / \partial z) (e n_e)^{-1}$ in cylindrical coordinates. Where the poloidal current flows outward – $J_z > 0$ – the toroidal field will migrate toward lower densities. There the crust has a smaller shear modulus and is less able to balance magnetic shear stresses. The net effect is to excavate the twist in the poloidal field from the crust, on the timescale $t_{\text{Hall}} = 2.4 \times 10^5 (R_6 / B_{\phi,15}) \rho_{14}^{5/3}$ yr at a radius $R = R_6 \times 10^6$ cm and density $\rho_{14} \times 10^{14}$ g cm $^{-3}$.

The Hall effect has different consequences in the fluid core. In a liquid that is stratified parallel to gravity \mathbf{g} , Hall drift creates unbalanced magnetic stresses. In particular, hall waves do not exist as propagating modes in the high frequency limit, $k|d \ln \rho/dz|^{-1} \gg 1$. To show this, note that the Hall term can only be cancelled by a hydrodynamic displacement

satisfying $v_z = 0$. This condition is satisfied if \mathbf{v}_{Hall} has no vertical component, i.e., if $J_z = 0$. A simple example is a finite-amplitude field variation $\mathbf{B}' = \mathbf{B}'_0 \exp(i\mathbf{k} \cdot \mathbf{x})$ superimposed on a uniform background field \mathbf{B}_0 . Magnetostatic equilibrium requires that \mathbf{B}' be linearly polarized, and that $(\mathbf{B}'_0 \times \mathbf{k}) \cdot \mathbf{g} = 0$, which implies in turn $J_z = 0$.

On larger scales, the Hall term in the induction equation generally *cannot* be cancelled off by such a hydrodynamic displacement field in the fluid core.¹ Hall drift evolves the magnetic field into a new configuration of equal total energy (GR), but if the field is initially an a stable configuration then all displacements satisfying $v_r = 0$, $\nabla \cdot \mathbf{v} = 0$ increase its energy. In fact, the new configuration will generally have a *higher* energy than some neighboring configuration into which it can relax. In what follows, we make the reasonable assumption that this excess energy is converted to heat on a timescale much less than $\sim 10^3$ yrs.

The next step is a prescription for the *hydrodynamic* response of the fluid interior to this diffusive motion. We define a characteristic poloidal magnetic field B_P , toroidal field $B_\phi = O(10)B_P$, and tilt angle α between the poloidal current and the direction of gravity at the center of each toroidal loop. There is a characteristic tilt, $\alpha \sim B_P/B_\phi$, below which the field is able to largely unwind through differential rotations of fluid shells confined to gravitational equipotential surfaces (Fig. 2 of Thompson & Duncan 2001). Hence changes in α can cause unwinding of the toroidal field at the rate $dB_\phi/dt = -(B_\phi/\alpha) |d\alpha/dt|$. On the other hand, microscopic transport of the field on a timescale τ causes changes in α at a rate $d\alpha/dt \sim \pm\tau^{-1}$. Thus we evolve the simple one-field model

$$\frac{dB_\phi}{dt} = -\frac{B_\phi}{\alpha} \left[\frac{1}{t_{\text{amb}}(B_\phi)} + \frac{1}{t_{\text{Hall}}(B_\phi)} \right]. \quad (2)$$

Unwinding of the field does not require any change in B_P , and the associated transport time is much longer when $B_P \ll B_\phi$. Hence we only evolve B_ϕ .

A net change in winding of the core magnetic field must be accompanied by a torsional deformation of the stellar crust. The energy deposited in an area A of the crust by twisting it through an angle θ is $\sim \theta^2 \int \mu dV \sim 5 \times 10^{40} (\theta/0.001)^2 (A/100 \text{ km}^2)$ ergs. (Here $\mu = 1.1 \times 10^{30} \rho_{14}^{0.8}$ is the crustal shear modulus; Strohmayer et al. 1991.) During a concentrated episode of SGR activity, when hundreds of ~ 0.1 -s X-ray bursts are emitted, this process might be repeated $\sim \theta^{-1}$ times, and the net crustal heat deposition would be $\sim 1000 (\theta/0.001)^{-1}$ times larger. A giant flare evidently involves a single readjustment through a much larger angle.

¹Mestel (1956) has argued that Hall drift of an axisymmetric poloidal magnetic field will excite a torsional Alfvén wave in a fluid star. However, such a field configuration has a special symmetry (radial current $J_r = 0$) and the above argument indicates that the Hall drift will instead be cancelled by a compensating hydrodynamic motion.

A toroidal magnetic field confined to the crust will, in a first approximation, evolve independently from that in the core. The net angle through which a radial poloidal field is twisted (across one vertical density scale height) is limited by the finite yield strain ψ of the crust, $\Delta\phi_B = (\ell_\rho/R)(B_\phi/B_z) \leq (4\pi\mu/B_z^2)\psi$. This sets an upper bound $B_\phi \leq 7 \times 10^{15} B_{z,14}^{-1}(\psi/10^{-3})R_6$ G. Integrating the above Hall equation for B_ϕ , under the assumption that inhomogeneities in the winding of the field relax completely in the deep crust after each yielding event, gives $B_\phi/B_{\phi,0} = [1 + t/t_{\text{Hall}}(B_{\phi,0})]^{-1}$. The corresponding heating rate, integrated over depth z , $2 \times 10^{33} B_{\phi,15}^3 A_{13} R_6^{-1} [1 + t/t_{\text{Hall}}(B_{\phi,0})]^{-3}$ ergs s $^{-1}$, is constant as $t \rightarrow 0$ and scales as t^{-3} at $t \gg t_{\text{Hall}}(B_{\phi,0})$. We will revisit the interplay between radial currents and Hall drift elsewhere in more detail.

3. Coupled Thermal Evolution and Field Decay

The thermal evolution of the star is followed using a relativistic model constructed from the Tolman-Oppenheimer-Volkoff equations and the parametrized equation of state of Prakash, Lattimer, and Ainsworth (1988) with intermediate compressibility ($K = 240$ MeV) and a mass low enough that direct URCA cooling can be neglected ($M = 1.35 M_\odot$). (We note that more recent EOS indicate the absence of direct URCA cooling for much larger masses; Akmal, Pandharipande, and Ravenhall 1998.) We are interested here in baseline thermal evolution, averaged over a timescale long compared with the conduction times across the crust, which is more than two orders of magnitude shorter than the spindown ages of the SGRs and AXPs ($P/2\dot{P} \gtrsim 10^3$ yr). The calculation therefore takes into account the effects of continuous modes of magnetic field decay.

We calculate the net neutrino luminosity L_ν by integrating the emissivities due to the modified URCA reaction ($\{n, p\} + n \leftrightarrow \{n, p\} + p + e^- + \bar{\nu}_e$), nucleon bremsstrahlung emission ($n + n \rightarrow n + n + \nu + \bar{\nu}$, etc.) and neutron Cooper pair emission ($n + n \rightarrow (2n) + \nu + \bar{\nu}$); evolving the magnetic field according to eq. (2) using the volume-averaged modified-URCA rate in t_{amb} ; calculating the luminosity $L_X = 4\pi R_{\text{NS}}^2 e^{2\phi(R_{\text{NS}})} \sigma_{\text{SB}} T_s^4$ ($\phi(r)$ = gravitational potential) in thermal surface X-ray emission from the relation between core temperature and surface temperature T_s detailed below; and, finally, evolving the (redshifted) core temperature $T_c = e^{\phi(r)} T(r)$ in the isothermal approximation by balancing the net cooling luminosity with the rate of loss of magnetic energy from the volume V of the star,

$$\langle C_V \rangle \frac{dT_c}{dt} = -\frac{1}{V} (L_\nu + L_X) + e^{2\phi(R_{\text{NS}})} \frac{B_\phi}{4\pi} \frac{dB_\phi}{dt}. \quad (3)$$

Balancing only the last term with the modified-URCA emissivity, one finds $\Delta\mu \sim B^2/8\pi n_e \sim \alpha(k_B T_c)$. There are finite- $\Delta\mu$ corrections to the URCA rates (Reisenegger 1995), but these

are generally less important than the corrections due to nucleon pairing when $\alpha \ll 1$.

The heat flux emerging through the surface of a magnetar depends on the relation between the surface effective temperature T_s and the temperature T_c in the deep crust. This relation has been calculated (Van Riper 1988; Heyl & Hernquist 1997; Potekhin and Yakovlev 2001) for a magnetized atmosphere in which the ions form a non-ideal gas. At the surface temperature characteristic of SGRs and AXPs ($k_B T_{\text{bb}} \sim 0.4\text{-}0.5 \text{ keV}$; Özel, Psaltis, & Kaspi 2001) one however expects heavy ions (e.g. iron) to be condensed into long molecular chains (Lai and Salpeter 1997). The density is then large even close to the surface and can be estimated by minimizing the sum of the Coulomb and electron degeneracy energies in a Wigner-Seitz cell:² $\rho(0) \simeq 1.8 \times 10^7 (Y_e/0.5)^{-1} (Z/26)^{2/5} (B/10^{15} \text{ G})^{6/5} \text{ g cm}^{-3}$.

The transmission of heat through the atmosphere of a neutron star with zero surface magnetic field is controlled by a sensitivity strip of a lower density $\rho \sim 10^5 - 10^6 \text{ g cm}^{-3}$ (e.g. Potekhin & Yakovlev 2001). Fig. 1 shows the surface temperature of a neutron star with normal core neutrons and protons (transition temperatures $T_{c,n} = T_{c,p} = 0$) using this standard envelope model. We have also included the effect of ambipolar diffusion of an internal toroidal field ($B_\phi = 3, 5 \times 10^{15} \text{ G}$), using eq. (2) and the ambipolar diffusion timescale t_{amb} tabulated in eqs. (58), (59) of GR. (See also Heyl & Kulkarni 1998.)

The heat flux is higher in a second envelope model which we have constructed for a condensed iron surface layer in a 10^{15} G magnetic field. The best power-law fit is $T_s/g_{14}^{1/4} = 4.0 \times 10^6 \text{ K} (T_c/10^9 \text{ K})^{1/2} [2.9 \times 10^6 \text{ K} (T_c/10^9 \text{ K})^{1/4}]$ for T_c greater than [less than] $2.8 \times 10^8 \text{ K}$, and gravity $g = g_{14} \times 10^{14} \text{ cm s}^{-2}$. The integration of dT/dz over depth z idealizes the electrons as a (locally) uniform fermi gas, and employs the thermal conductivity tabulated by Potekhin (1999). The ideal finite- T electron equation of state is supplemented by a correction for the (negative) Coulomb pressure in the solid phase, $P = P_e - P_e(0)[n_e/n_e(0)]^{4/3}$, where $P_e(0)$ and $n_e(0)$ are the electron degeneracy pressure and density at zero total pressure P .

Much of the thermal resistance is localized where the electrons are 1-dimensional, with fermi momentum $p_{Fe} \sim m_e c$ (density $\rho = Y_e m_p e B p_{Fe} / 2\pi^2 \hbar^2 c \sim 10^8 B_{15} \text{ g cm}^{-3}$) and where the melting temperature is $1 \times 10^8 (Z/26)^{5/3} B_{15}^{1/3} \text{ K}$. Thus at high T_c the sensitivity strip lies in a Coulomb liquid layer below the solid surface; whereas at low T_c (and large Z) it lies within the solid. In the solid, the electrons are nearly degenerate and heat is transported by conduction electrons within a narrow energy range $\sim k_B T$ near the fermi surface. The scalings for $T_s(T_c)$ are easily derived by approximating the conductivity as being due to phonon scattering (in the solid) or Coulomb scattering (in the liquid), with all the electrons in the lowest Landau state. This analytic model gives $T_s^4 \propto B_s^{1/5} Z^{-3/5}$ at high T_c , and

²Here Y_e is the electron fraction and Z the nuclear charge.

$T_s^4 \propto B_s$ at low T_c . To correct for the lower opacity of the extraordinary mode near the condensed surface, we show $2^{1/4}$ times the effective temperature. Since there is evidence for complicated multipolar structure in the surface magnetic field of some SGRs (Feroci et al. 2001), B_s is a characteristic surface field without any dipole structure.

Our numerical results are plotted in Figs. 1 and 2. In sum:

- i) Steady heating of the stellar interior by a $\sim 3 \times 10^{15}$ G magnetic field increases $\log_{10}(T_s)$ by ~ 0.2 if the core neutrons and protons are normal. Proton pairing suppresses the rate of charged-current weak interactions and therefore the rate of the irrotational mode of ambipolar diffusion; in which case Hall drift makes a similar contribution to the decay of the core magnetic field before the core superfluid transition, and dominates thereafter.
- ii) If the peak pairing temperature $T_{c,n} \gtrsim 6 \times 10^8$ K, the drop in T_s is gradual and occurs earlier than ~ 100 years; but if $T_{c,n} \lesssim 5 \times 10^8$ K, then this drop is sharper and occurs in the observed age range of SGR/AXP activity. Magnetic dissipation can delay the time of the pairing transition by an order of magnitude. It also delays (and makes sharper) the transition to photon-dominated cooling. If the internal B-field is much stronger than 10^{14} G, and its coherence length is large (~ 10 km), then continuous Hall decay (which is not temperature sensitive) will keep the surface warm up to an age of several $\times 10^5$ yrs (redshifted temperature $T_s^\infty = T_s e^{\phi(R_{\text{NS}})} \sim 1.5 \times 10^6$ K). Strong intermittency in the rate of Hall decay would allow the core to cool off more rapidly in between magnetic ‘flares’, due to the strong temperature dependence of the neutrino emissivities, and the temperature evolution would be intermediate between the dashed and solid curves in Fig. 2.
- iii) The thermal evolution with a condensed Fe atmosphere gives T_s^∞ within a factor $\sim 1.3\text{--}1.5$ of those measured in the thermal components of AXP spectra ($kT_{\text{bb}} \simeq 0.4\text{--}0.5$ keV) at an age of $\sim 10^3\text{--}10^4$ yrs. A relatively thin light-element layer will harden the thermal peak by this amount, compared with a pure black body (e.g. Lloyd, Hernquist, and Heyl 2003). If the surface field is $\sim 10^{15}$ G, then L_X is generally less than 10^{35} erg s $^{-1}$, consistent with some AXP sources but not all (e.g. Özel et al. 2001). Recalculating the cooling models with a lighter element (carbon) surface layer shows a factor $\sim 3\text{--}4$ increase in thermal transparency at early times – but not below $T_s \sim 4 \times 10^6$ K, so that the photon cooling time does not change significantly. Heating by an external current may also not be negligible: the power needed to force a current of ions and electrons through a twisted magnetosphere with a constant equatorial pitch B_ϕ/B_θ is $L_X \sim 3 \times 10^{35} (B_{\text{pole}}/10^{14} \text{ G})(B_\phi/B_\theta)$ ergs/s (Thompson et al. 2002).

4. Timing Noise and Core Neutron Superfluidity

Phase-resolved X-ray timing of SGRs 1806–20 and 1900+14 have revealed a broad spectrum of timing noise (Woods et al. 2002). At short time intervals ($\Delta t \sim 3 \times 10^4$ s) large phase offsets ($\Delta\phi \sim 0.3$ cycles) are sometimes observed in the X-ray pulses, which prevent phase-connected timing. These offsets correspond to stochastic shifts in frequency of magnitude $\Delta\nu/\nu \sim 10^{-4}$. The alternative is an enormous increase in frequency derivative by $\sim 10^2$ ($\Delta\dot{\nu} \sim 2\Delta\phi/\Delta t^2 \sim 10^{-9}$ s $^{-2}$). Hence the effect appears to be due to the absorption and release of angular momentum by an internal superfluid component. The lack of obvious classical post-glitch relaxation behavior, and the magnitude of the timing residuals, lead us identify a *superfluid core* as the reservoir of angular momentum. Indeed, no obvious correlation exists between this timing noise and the observation of long-term torque variations, bright X-ray outbursts, or large changes in persistent X-ray flux that would be associated with deformations of the crust.

Timing noise of this amplitude is absent in radio pulsars, and its presence in magnetars is strongly correlated with *overall* activity as a burst source, and with a spectrally hard persistent X-ray emission. Part of this correlation could result from the reduction in interior temperature (by a factor ~ 5) coinciding with the pairing transition of the neutrons, which would make the crust more brittle; and from a reduction in surface cooling rate in comparison with the power dissipated by external currents.

In a slowly rotating magnetar, the outward motion of the vortices is constrained by the magnetic field, due to the large energetic barrier to the crossing of vortices and superconducting fluxoids (e.g. Ruderman et al. 1998). Slow fluctuations in the field of amplitude $\Delta B/B \sim (I_{\text{sf}}/I)^{-1} \Delta\nu/\nu \sim 10^{-4} (I_{\text{sf}}/I)^{-1}$, with some amplitude perpendicular to the axis of rotation, would provide the necessary perturbation to the superfluid. If such fluctuations are to occur over many ($> 10^4$) core Alfvén-crossing times, the field configuration must be metastable, and nearly degenerate in energy with others that differ by one part in $\sim 10^4$. This is expected if the core field has relaxed significantly from an initial equilibrium state.

5. Conclusions and Observational Tests

Several degrees of freedom strongly influence the thermal and spectral evolution of a magnetar: i) the strength of its internal magnetic field; ii) the temperature at which core neutrons become superfluid; iii) the transmissivity of its thermal envelope; and iv) the configuration of its internal magnetic field and the equilibrium states through which this field moves. Before a core superfluid transition, thermal luminosities up to $\sim 10^{35}$ ergs/s

are possible if the surface magnetic field is $\sim 10^{15}$ G; thereafter, the neutrino emissivity rises dramatically due to Cooper pair cooling, and thermal emission powered by internal Hall decay can continue at a level $\lesssim 10^{34}$ ergs/s beyond an age of $\sim 10^5$ yrs. We infer that magnetar candidates which show transitions to/from such low luminosity states have magnetic fields of intermediate strength and/or superfluid cores. We have also argued that the observation of fast timing noise in SGRs 1900+14 and 1806–20 provides direct evidence for a superfluid neutron core. The highly non-thermal persistent X-ray emission of these sources must be powered mainly by external currents; but a thermal seed could be provided by internal heating. (The AXP with the hardest X-ray spectrum and noisiest spindown, 1E 1048.1–5937, also has a relatively low blackbody luminosity, less than 10^{34} ergs/s; Özel et al. 2003.) SGR 0526–66 has remained X-ray bright since its last observed outburst in 1983 (Kulkarni et al. 2003) and has a high luminosity $\sim 7 \times 10^{35}$ erg/s: either $B \gg 10^{15}$ G at its surface, or most of its emission continues to be powered by external currents (in spite of the relatively soft X-ray spectrum). Detailed timing measurements of this source would provide valuable diagnostics of its interior state.

We thank Lars Bildsten, Vicky Kaspi, Shri Kulkarni, Bennett Link, and Peter Woods for conversations. PA is an AAPF NSF fellow, AC is a Hubble Fellow, and CT acknowledges the support of the NSERC of Canada.

REFERENCES

Akmal, A., Pandharipande, V. R., & Ravenhall, D. G. 1998, Phys. Rev. C, 58, 1804
Colpi, M., Geppert, U., & Page, D. 2000, ApJ, 529, L29
Feroci, M., Hurley, K., Duncan, R. C., & Thompson, C. 2001, ApJ, 549, 1021
Flowers, E. & Ruderman, M. A. 1977, ApJ, 215, 302
Gavriil, F. P., Kaspi, V. M., & Woods, P. M. 2002, Nature, 419, 142
Goldreich, P. & Reisenegger, A. 1992, ApJ, 395, 250 (GR)
Haensel, P., Urpin, V. A., & Iakovlev, D. G. 1990, A&A, 229, 133
Heyl, J.S. & Hernquist, L. 1998, MNRAS, 300, 599
Heyl, J. S. & Kulkarni, S. R. 1998, ApJ, 506, L61

Hurley, K. 2000, [astro-ph/9912061](#)

Ibrahim, A. et al. 2003, preprint ([astro-ph/0310665](#))

Kaspi, V. M. et al. 2001, *ApJ*, 558, 253

Kaspi, V. M. et al. 2003, *ApJ*, 588, L93

Kouveliotou, C. et al. 2003, *ApJ*, 596, L79

Kulkarni, S. R. et al. 2003, *ApJ*, 585, 948

Lai, D. & Salpeter, E. E. 1997, *ApJ*, 491, 270

Lloyd, D. A., Hernquist, L., & Heyl, J. S. 2003, *ApJ*, 593, 1024

Mestel, L. 1956, *MNRAS*, 116, 324

Özel, F., Psaltis, D., & Kaspi, V. M. 2001, *ApJ*, 563, 255

Pethick, C. J. 1992, Structure and Evolution of Neutron Stars, 115

Potekhin, A.Y. 1999, *A&A*, 351, 787

Potekhin, A.Y. & Yakovlev, D.G. 2001, *A&A*, 374, 213

Prakash, M., Lattimer, J. M., & Ainsworth, T. L. 1988, *Phys. Rev. Lett.*, 61, 2518

Reisenegger, A. 1995, *ApJ*, 442, 749

Reisenegger, A. & Goldreich, P. 1992, *ApJ*, 395, 240

Ruderman, M., Zhu, T., & Chen, K. 1998, *ApJ*, 502, 1027

Strohmayer, T. et al. 1991, *ApJ*, 375, 679

Tayler, R. J. 1973, *MNRAS*, 161, 365

Thompson, C. & Duncan, R. C. 1996, *ApJ*, 473, 322

Thompson, C. & Duncan, R. C. 2001, *ApJ*, 561, 980

Thompson, C., Lyutikov, & Kulkarni 2002, *ApJ*, 574, 332

Torii, K. et al. 1998, *ApJ*, 503, 843

van Riper, K. A. 1988, *ApJ*, 329, 339

Woods, P. M. et al. 2002, *ApJ*, 576, 381

Yakovlev, D. G., Kaminker, A. D., Gnedin, O. Y., & Haensel, P. 2001, *Phys. Rep.*, 354, 1

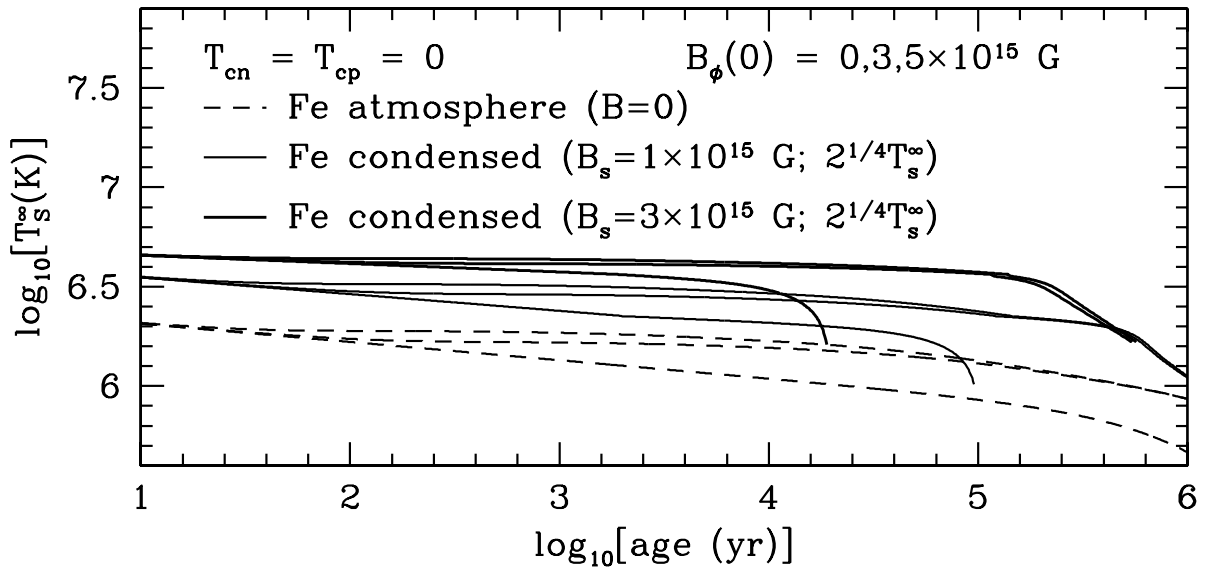


Fig. 1.— Surface temperature (redshifted) as a function of age, for a $1.35M_\odot$ neutron star with normal neutrons and protons. (Upper two curves in each set correspond to stars with internal heating mainly by ambipolar diffusion.) B_s is the surface field, which is assumed to be constant in time, and B_ϕ the internal toroidal field (which may be stronger). See text for the description of the envelope models. The factor of $2^{1/4}$ corrects for surface emission dominated by the extraordinary polarization mode.

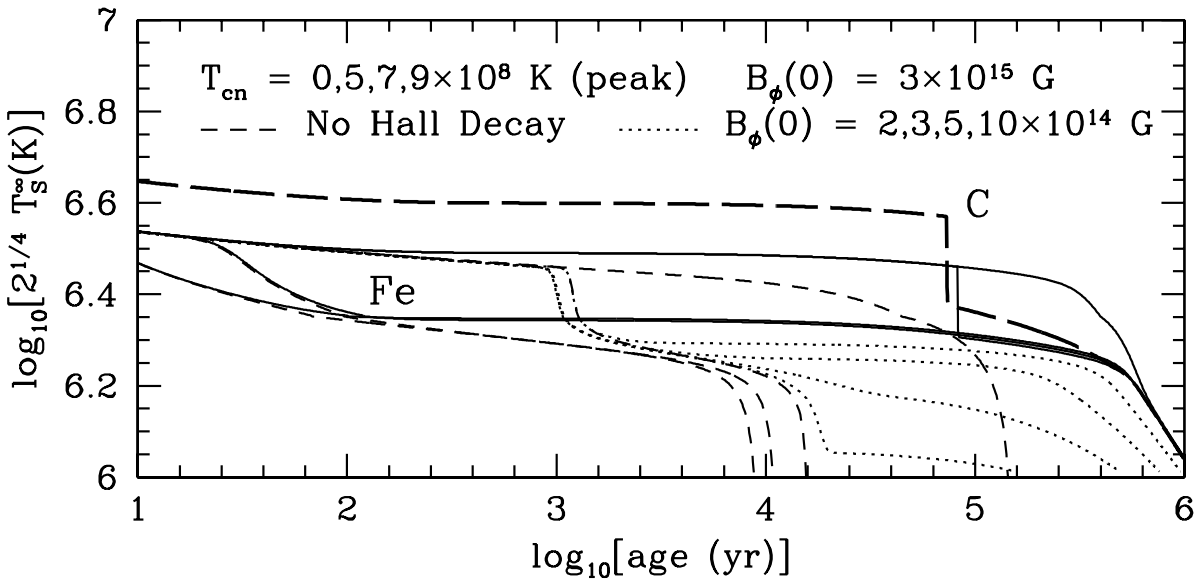


Fig. 2.— Same but for a condensed iron envelope, superconducting core protons ($T_{c,p} = 5 \times 10^9$ K), and various peak pairing temperatures for the core neutrons. The distribution of critical temperature $T_{c,n}$ with density is taken to be $T_{c,n} = T_{c,n}(\text{peak}) \exp[-(\rho_{14} - 5)^2/\rho_{14}^2]$. Smooth declines in X-ray flux at $t > 10^{4-5}$ yrs occur when surface cooling begins to dominate. Sharper drops signal a transition to core superfluidity. Those occurring at $t < 100$ yrs correspond to $T_{c,n}(\text{peak}) = 9, 7 \times 10^8$ K; and at $t \sim 10^5$ yrs to $T_{c,n}(\text{peak}) = 5 \times 10^8$ K. Solid curves ($B_s = 10^{15}$ G) include the effects of Hall decay. Dashed curves do not, and ordered from left to right correspond to $T_{c,n}(\text{peak}) = 9, 7, 5, 0 \times 10^8$ K. Notice that the superfluid transition is greatly delayed for $T_{c,n} = 5 \times 10^8$ K. Dotted curves show weaker magnetic fields, $B_s = B_\phi(0) = 2 - 10 \times 10^{14}$ G and $T_{c,n} = 5 \times 10^8$ K. Finally, the top dashed curve shows enhanced cooling through a condensed carbon envelope (density $\leq 1 \times 10^{10}$ g cm $^{-3}$) with $B_s = 1 \times 10^{15}$ G, $B_\phi(0) = 3 \times 10^{15}$ G, and $T_{c,n} = 5 \times 10^8$ K.